Nonlinear Model Predictive Control of High Purity Distillation Columns for Cryogenic Air Separation

Zhongzhou Chen, Michael A. Henson, *Senior Member, IEEE*, Paul Belanger, and Lawrence Megan

Abstract—High purity distillation columns are critical unit operations in cryogenic air separation plants that supply purified gases to a number of industries. We have developed a nonlinear model predictive control (NMPC) strategy based on the assumption of full-state feedback for a prototypical cryogenic distillation column to allow effective operation over a wide range of plant production rates. The controller design was based on a reduced-order compartmental model derived from detailed mass and energy balances by exploiting time-scale separations. Temporal discretization of the compartmental model produced a very large set of nonlinear differential and algebraic equations with advantageous sparsity properties, enabling online solution of the NMPC problem. The synergistic combination of several real-time implementation techniques were found to be essential for further reducing computation time and allowing reliable solution within the 2-min controller sampling interval. Closed-loop simulation studies demonstrated the performance advantages of NMPC compared to linear model predictive control technology currently used in the air separation industry.

Index Terms—Nonlinear model predictive control (NMPC), process control, real-time optimization, reduced-order modeling.

I. INTRODUCTION

CRYOGENIC distillation is used to produce large quantities of purified nitrogen, oxygen, argon, and rare gases for the steel, chemical, food processing, semiconductor, and health care industries [1], [2]. Cryogenic distillation columns are operated at extremely low temperatures (-170 to $-190°$C) to separate air components according to their different boiling temperatures. Purified streams are produced in liquid and/or gaseous states for transportation to end-users. The major operating cost associated with cryogenic air separation plants is electricity. Because the domestic consumption of electricity by industrial gas producers is over \$1 billion per year, small improvements in process control have the potential to result in substantial economic benefits.

 Current state-of-the-art control technology in the air separation industry is based on linear dynamic models and linear model predictive control [3], [4]. Despite the very high product purities required, linear control technology has proven to be successful because cryogenic distillation columns traditionally operate over a small range of production rates. Deregulation of the electric utility industry is expected to lead to frequent and unpredictable changes in the cost of electricity, which will mandate fundamental changes in the operating philosophy of air separation plants. Large changes in production rate and more frequent startups/shutdowns will be required to take full advantage of time-varying utility rates. One possible strategy is to maximize production when electricity is relatively inexpensive and to minimize production when electricity costs are high. Column nonlinearities will become much more pronounced under these operating conditions, and some type of nonlinear control will be necessary to achieve satisfactory performance.

Nonlinear model predictive control (NMPC) is an extension of linear model predictive control, where a nonlinear model is used to describe the process dynamics [5]–[8]. A variety of numerical algorithms are available to solve the NMPC optimization problem. The simultaneous solution approach involves temporal discretization of the dynamic model equations to produce a set of nonlinear algebraic equations (AEs) that are posed as equality constraints in the NMPC optimization problem [9], [10]. The decision variables are current and future values of the manipulated inputs and state variables. Because control moves are generated by real-time solution of the resulting nonlinear program at each sampling time, computational effort is inextricably linked to the complexity of the controller design model.

Fundamental models of distillation columns are comprised of stage-by-stage mass and energy balances combined with vapor-liquid equilibrium relations expressed for each stage [4], [11]. A distillation column with N equilibrium separation stages and n chemical species can be modeled with $N(n + 2)$ nonlinear ordinary differential equations (ODEs) describing the species compositions, liquid and vapor flow rates, and temperature on each stage. The vapor phase and temperature dynamics usually are assumed to be fast, such that the corresponding ODEs are reduced to AEs. We have modeled the 59-stage cryogenic distillation column in this paper with 180 ODEs and 137 AEs. Such nonlinear dynamic models generally are viewed as being too complex to be effectively utilized for real-time control due to their high dimensionality. While advanced solution techniques have been shown to allow the application of NMPC to distillation column models of moderate complexity [12], [13], there remains considerable motivation to develop reduced-order dynamic models that provide a more favorable tradeoff between prediction accuracy and optimization effort. The derivation of reduced-order column distillation models

Z. Chen and M. A. Henson are with the Department of Chemical Engineering, University of Massachusetts, Amherst, MA 01003-9303 USA (e-mail: chen-zhongzhou@gmail.com; henson@ecs.umass.edu).

P. Belanger and L. Megan are with the Process and Systems Research and Development, Praxair, Inc. Tonawanda, NY 14051-7891 USA (e-mail: Paul_Belanger@praxair.com; Larry_Megan@praxair.com).
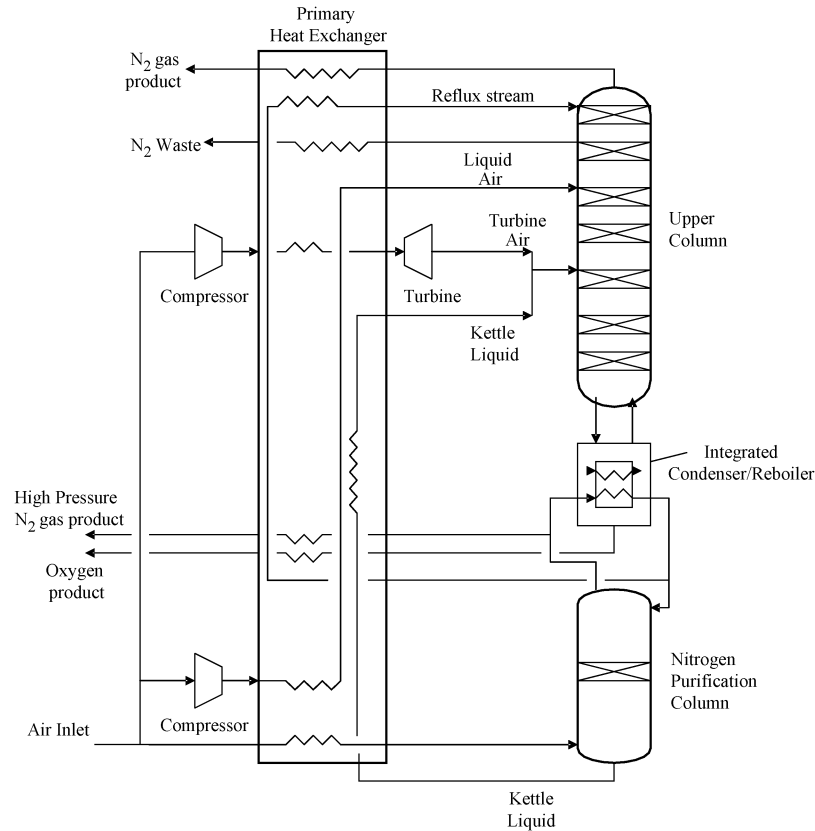
Fig. 1. Schematic diagram of a typical double column air separation plant.

from more detailed stage-by-stage models has received considerable attention [14]–[19].

In this paper, a NMPC strategy based on a reduced-order model of a cryogenic distillation column is developed and evaluated through simulation studies. The column has multiple feed and product withdrawal streams, further complicating the design of an effective control system. Our main contribution is to present the combination of reduced-order modeling, temporal discretization, nonlinear programming, and real-time implementation techniques required to develop an industrially realizable NMPC controller. We have previously derived a detailed stage-by-stage balance model to serve as a surrogate plant in our simulation studies and to provide a rigorous basis for reduced-order model development [20]. As part of this work, a nonlinear compartmental model [21] was derived by exploiting time-scale separations in the full-order model. Here we show that the temporally discretized compartmental model has increased sparsity as compared to the full-order model, which facilitates efficient solution of the NMPC problem. A number of real-time implementation strategies are employed to achieve converged NMPC solutions within the 2-min controller sampling interval. Closed-loop simulations are conducted under the assumption of full-state feedback and noise-free measurements to compare the performance of the NMPC controller to a conventional linear model predictive controller and to assess the potential utility of NMPC technology for cryogenic and other high-purity distillation columns.

II. DISTILLATION COLUMN MODELING

The scope of this work was limited to the upper distillation column of a double column air separation plant (Fig. 1). The upper column has 59 separation stages including the reboiler, and seven liquid distributors are placed throughout the column to improve the flow characteristics of the descending liquid. The column directly receives two air feed streams (liquid air on stage 18 and turbine and kettle air on stage 35) following gas compression and expansion that achieves the cryogenic temperatures necessary for separation. The upper column is coupled to the lower nitrogen purification column through the integrated condenser/reboiler and the reflux stream (entering stage 1) obtained from the overhead of the lower column. The nitrogen product is withdrawn from stage 1, and a gaseous nitrogen waste stream is withdrawn from stage 10. The oxygen product is withdrawn from the integrated condenser/reboiler (stage 59).

A. Full-Order Model

We previously derived a stage-by-stage mass and energy balance model of the upper column to provide the basis for compartmental model development and to serve as the plant in our simulation studies [20]. This full-order model was based on the following assumptions: 1) ternary gas mixture consisting of nitrogen, oxygen, and argon; 2) negligible vapor phase holdups; 3) ideal vapor phase behavior; 4) fast temperature dynamics; 5) linear pressure profile across the column; 6) complete mixing

of the vapor and liquid streams entering the feed stages; and 7) constant reboiler medium temperature. The model was comprised of dynamic mass balances and a steady-state energy balance on each stage combined with an activity coefficient model to account for nonideal liquid phase behavior. Steady-state mass and energy balances were used to model mixing of the feed streams with internal vapor and liquid streams. Each liquid distributor was modeled as a separation stage with a very small separation efficiency (5%) to account for the effect of its large liquid holdup on column dynamics.

The complete upper column model consisted of 180 ODEs and 137 AEs with the following unknowns for each stage i: oxygen and argon mole fractions $(x_{O_2,i}, x_{Ar,i})$, liquid and vapor molar flow rates (L_i, V_i), and temperature (T_i). The matlab code ode15s was used to solve the differential-algebraic equation (DAE) model. The DAE model was index 1 due to the use of steady-state energy balances. If dynamic energy balances were used, the DAE model would be index 2 and column simulation would be considerably more difficult. Nitrogen compositions were computed from oxygen and argon compositions by noting that the three mass fractions sum to unity on any stage. To avoid the additional complexity of rigorous lower column modeling, simple linear models were developed to account for the effects of the lower column on the upper column. An Aspen Dynamics simulation of the lower column [22] was used to generate dynamic data for step changes in the air inlet flow rate to the plant assuming a constant condenser (warm side) temperature in the integrated condenser/reboiler (Fig. 1). This assumption was valid because the upper column pressure and product composition did not vary enough to impact the boiling side temperature. The simulation data was used to identify step response models with the air inlet flow rate as the input variable and each variable that affected the upper column as an output variable. These linear models were used to propagate the effects of air flow rate changes on the lower column to the upper column.

B. Compartmental Model

We have developed compartmental models of high purity distillation columns in cyrogenic air separation plants [20], [22]. While other nonlinear reduced-order modeling techniques have been developed for distillation columns [15], [16], [23], the main advantages of compartmental modeling are that the physicochemical features of the detailed column model are retained and that temporal discretization yields a sparse NMPC problem amenable to real-time solution. Compartmental models are derived directly from stage-by-stage balance models by dividing the column into a small number of sections termed compartments [21], [24]. A dynamic model of each compartment is developed by combining stage-by-stage balances with overall balances over the entire compartment. If the number of stages in the compartment is sufficiently large and each stage has a comparable liquid holdup, then the overall dynamics of the compartment are much slower than the dynamics of any individual stage within the compartment. This time-scale separation allows the compartment dynamics to be approximated with the ODEs for a representative stage within the compartment whose holdup is equal to the total

TABLE I
EQUATIONS COMPRISING THE FULL-ORDER AND COMPARTMENTAL MODELS

Model	Differential Variables	Algebraic Variables
Full-Order	180	137
15 compartment	48	269
9 compartment	30	287
5 compartment	18	299

compartment holdup [21]. Due to their relatively fast dynamics, the balance equations for other stages within the compartment are reduced to AEs through singular perturbation arguments [25].

We conducted a detailed compartmental modeling study for the upper column of a cryogenic air separation plant [20]. To examine the effect of compartmentalization on reduced-order model complexity and accuracy, three schemes were investigated: 15 compartments—a separate compartment was defined for the reboiler, each distributor, and the equilibrium stages located between adjacent distributors; nine compartments—distributors were lumped together with equilibrium stages such that only a single compartment was located between any two feed and/or product streams; and five compartments—the reboiler was treated as a single compartment, while the other compartments contained a single feed and withdrawal stream located at the first stage of the compartment. We found that the nine-compartment model provided the best compromise between model complexity and prediction accuracy relative to the full-order model. The interested reader should consult our previous publications [20], [22] for additional details on these results and the compartmental modeling procedure.

As compared to the full-order model, the compartmental models are comprised of relatively few ODEs representing the overall compartment dynamics and a large number of AEs derived from the dynamic stage balances (Table I). NMPC simultaneous solution methods require that both the differential and algebraic variables be included as decision variables and that temporally discretized versions of the equations be posed as equality constraints [9]. The AEs can be represented such that the equations at each temporal node point depend only on variables at the same node point. We discretize the ODEs using collocation on finite elements [10], producing equations at each node point that depend on all the variables within the same finite element. Therefore, the conversion of differential equations to algebraic equations through compartmentalization produces sparser Jacobian and Hessian matrices and offers the potential for more efficient solution of the NMPC problem. The most favorable compartmentalization scheme for NMPC is determined by the tradeoff between prediction accuracy and computational efficiency, as discussed in the next section.

III. NONLINEAR MODEL PREDICTIVE CONTROLLER

A. Controller Formulation

The full-order column model and the reduced-order compartmental models are DAE systems of the form

$$\frac{dx}{dt} = f(x, y, u, p)$$
$$0 = g(x, y, u, p) \qquad (1)$$

TABLE II
INPUT AND OUTPUT VARIABLES FOR MODEL PREDICTIVE CONTROL

Variable	Definition	Symbol	Units	Nominal Value
u_1	Total air feed flowrate	F_{air}	lb/hr	
u_2	Liquid air feed flowrate	F_{LA}	lb/hr	
u_3	Turbine air feed flowrate	F_{TA}	lb/hr	
u_4	Liquid Nitrogen addition flowrate	F_{LNADD}	lb/hr	
u_5	Gaseous oxygen production rate	F_{gO_2}	lb/hr	
y_1	Log transformed N_2 waste composition	$\ln(y_W)$	–	
y_2	Log transformed O_2 product purity	$-\ln[100(1 - y_{O_2})]$	–	

where $x(t)$ are the differential variables, $y(t)$ are the algebraic variables, $u(t)$ are the manipulated input variables, and p are constant model parameters. NMPC involves repeated online solution of the following nonlinear optimization problem to generate the control moves

$$\min_{u} \quad \Phi(x, y, u, p)$$
$$\text{s.t.} \quad \frac{dx}{dt} = f(x, y, u, p)$$
$$0 = g(x, y, u, p)$$
$$0 \leq h(x, y, u, p)$$
$$x|_{t=t_0} = x_0 \tag{2}$$

where Φ is the objective function used to measure controller performance. The solution is constrained by the DAE model, inequality constraints on the input and output variables, and the initial state. In this paper, we assumed that the state vector is measurable to determine the upper limits of achievable NMPC performance. We intend to present output feedback results in which the NMPC controller is combined with a nonlinear receding horizon state estimator [26], [27] in a future publication. The NMPC formulation does not contain specific features such as endpoint constraints and terminal penalties that have been proposed to guarantee nominal closed-loop stability [7], [8]. We found through extensive simulation studies that the NMPC controller was stabilizing if the prediction horizon was chosen to be sufficiently large. Because endpoint constraints typically reduce the feasible domain and can dramatically increase computation time, we determined that their inclusion was both unnecessary and undesirable.

Numerical solution of the optimization problem (2) is difficult due to its continuous-time formulation and the presence of differential equation constraints. Consequently, we utilized a simultaneous solution strategy based on temporal discretization of the DAE model using Radau collocation on finite elements [9]. As compared to collocation across the entire prediction horizon, the use of finite elements allowed better approximation of steep concentration profiles and produced a much sparser NMPC problem amenable to real-time solution. Each finite element was chosen to have the same length as the sampling interval (2 min) to facilitate controller implementation. A single internal collocation point within each finite elements of produced an accurate solution when compared to the original model (1) simulated with the DAE solver DASSPK [28] (not shown). Because the introduction of an additional collocation point increased simulation time an order of magnitude while

only slightly improving solution accuracy, we used a single collocation point in our closed-loop simulations.

The objective function for the discretized problem was chosen as

$$\Phi = \sum_{j=1}^{N_o} \sum_{k=1}^{P} q_j \left(y_{j,k} - y_{j,k}^r \right)^2 + \sum_{j=1}^{N_i} \sum_{k=1}^{M} r_j \left(u_{j,k} - u_{j,k}^r \right)^2$$
$$+ \sum_{j=1}^{N_i} \sum_{k=1}^{M} s_j (u_{j,k} - u_{j,k-1})^2 \tag{3}$$

where $u_{j,k}$ and $y_{j,k}$ denote the jth input and output values, respectively, at time-step k; $u_{j,k}^r$ and $y_{j,k}^r$ represent the corresponding target values; q_j, r_j, and s_j are time-independent weighting coefficients that were chosen by trial and error to achieve good controller performance; N_i and N_o are the number of inputs and outputs, respectively; M is the control horizon over which the inputs are allowed to change; and P is the prediction horizon over which the optimization is performed. The upper column represents a nonsquare control problem with $N_i = 5$ and $N_o = 2$ (Table II). The controlled variables were chosen as the gaseous O_2 product purity y_{O_2} (stage 59) and the waste N_2 composition y_W (stage 10), which was more responsive to the inputs than the gaseous N_2 product purity (stage 1) and could be controlled at an appropriately chosen setpoint to provide regulation of the product purity. Due to their high purities, both outputs were subjected to partially linearizing logarithmic transformations (Table II) used by Praxair in their existing LMPC application. Although both outputs only must be controlled within prescribed limits (discussed below), we found that including explicit setpoints (y_j^r) in the objective function significantly improved NMPC performance by reducing the input degrees of freedom and producing more reasonable control moves.

The upper column has three independently adjustable air feed flow rates (Fig. 1). Accordingly, the first three inputs were chosen as the total air feed flowrate (entering the lower column), the liquid air feed flowrate (stage 18), and the turbine air feed flowrate (stage 35). As discussed earlier, the effects of the total air flowrate were propagated to the upper column using empirical linear models identified from an Aspen simulation model of the lower column. Stored liquid nitrogen can be introduced into the top of the upper column (not shown in Fig. 1) to generate large and rapid increases in the nitrogen product and waste compositions. Therefore, the fourth input was chosen as the flowrate of this liquid nitrogen stream. The fifth input was chosen as the gaseous O_2 production rate, which was adjusted by the controller to meet the specified demand (u_5^r). Both the

liquid air feed flowrate (u_2) and the liquid nitrogen flowrate (u_4) are relatively expensive inputs due to refrigeration costs associated with their production. Consequently, the controller was tuned with relatively large weights r_2 and r_4 such that these inputs were driven close to their target values whenever possible.

The objective function (3) was minimized subject to several types of equality and inequality constraints. The DAEs comprising the column model were temporally discretized using Radau collocation on finite elements to yield a large set of nonlinear algebraic equations constraints. The two outputs were constrained to remain within lower and/or upper limits chosen to satisfy product purity requirements

$$y_i^L \le y_{j,k} \le y_i^U \quad j=1,2; k=1,2,\ldots,P. \qquad (4)$$

Two types of constraints were imposed on the inputs: absolute constraints to ensure that the inputs remained within reasonable bounds and rate-of-change constraints to avoid highly aggressive control moves

$$u_{j,\min} \le u_{j,k} \le u_{j,\max} \quad j=1,\ldots,5; \ k=1,2,\ldots,M \quad (5)$$

$$\Delta u_{j,\min} \le u_{j,k} - u_{j,k-1} \le \Delta u_{j,\max}. \qquad (6)$$

A standard output disturbance model was used to eliminate steady-state offset resulting from plant-model mismatch. A nonlinear program (NLP) was formulated by treating both the manipulated input and state variables at each collocation point as optimization variables [10]. NLP infeasibilities due to the hard output constraints were handled by sequentially removing the constraints at the beginning of the prediction horizon until the smallest number of intervals at which the constraints must be removed to achieve feasibility was determined. However, the hard bounds used in our simulations were not sufficiently restrictive to generate controller infeasibilities. Very wide inequality constraints were placed on the state variables to ensure that the NLP solver remained in the appropriate solution space. These constraints had no effect on controller feasibility.

B. Real-Time Solution Strategy

The full-order model implemented in MATLAB served as the virtual plant for closed-loop simulations. The NMPC controller was implemented in AMPL, an advanced programming language for optimization model development and solution [29]. AMPL allowed the optimization model to be rapidly developed, enabled investigation of different NLP solvers, and provided analytical calculation of the Jacobian and Hessian matrices needed by the solvers. The MATLAB and AMPL codes exchanged information through Excel data files. We assumed that the state vector was measurable and that the measurements were not corrupted by noise to determine the upper limits of achievable NMPC performance.

The NMPC sampling time $\Delta t = 2$ min was chosen to be commensurate with sampling times commonly used for linear MPC control of cryogenic air separation columns. A prediction horizon of 240 min ($P = 120$) was chosen according to the model steady-state response time, which was approximately 4 h. The control horizon of 20 min ($M = 10$) was chosen to be as small as possible to reduce computation time while achieving

acceptable closed-loop performance. Other than the requirement that the input weights r_2 and r_4 be chosen to be relatively large to penalize large moves in the liquid air feed flowrate (u_2) and the liquid nitrogen flowrate (u_4), the controller weights (q_j, r_j, s_j) were chosen by a trial-and-error tuning procedure to obtain satisfactory performance of NMPC controllers based on the full-order and compartmental models. We found that a wide range of tuning parameters yielded closed-loop stability, so the tuning effort was focused on obtaining good performance for production rate changes. The tuning parameter values for each controller are not reported here for the sake of brevity.

The full-order column model contains 317 state variables representing the liquid phase composition, temperature, liquid holdup, and vapor flowrate on each stage. However, the model also contains many intermediate thermodynamic variables used to calculate activity coefficients, gas phase compositions, and enthalpies. The intermediate thermodynamic equations were posed as algebraic constraints in the NLP problem used for NMPC implementation. Because there are approximately six times the number of intermediate variables as state variables, the NLP had approximately 500 000 optimization variables and equality constraints that had to be solved at every time-step within the 2-min controller sampling interval. Our preliminary simulation results indicated that IPOPT [30] was better suited for this very large and highly sparse NLP problem than the popular solver CONOPT. However IPOPT sometimes required as much as 40 min of CPU time following a step change in the gaseous O_2 production rate demand, a factor of 20 times larger than that necessary for real-time implementation. While any computational delay has the potential to degrade controller performance, consistent convergence of the controller calculations within the sampling time is necessary for real-time implementation. If the controller did not return a fully converged solution within the 2-min sampling interval, then the partially converged solution available at that time was used. We found that closed-loop performance could be adversely and unpredictably affected by the use of partially converged solutions, with instability resulting if such solutions are used too frequently. Therefore, we made every effort to ensure that the controller consistently converged within the sampling interval. While faster converged solutions could be achieved with more powerful computers than our Pentium IV desktop machine and/or parallelization of the controller calculations, we instead sought to develop real-time implementation strategies that would reduce NMPC execution times on any computer platform.

We found that a combination of different implementation strategies were required to develop a NMPC controller capable of consistently returning converged control moves within the two sampling interval. Fig. 2 shows the impact of the seven strategies used on the NMPC execution time immediately following a particularly difficult step change in the gaseous O_2 production demand (u_5^r). The strategies were numbered according to their relative impact on the execution time, where strategy 1 produced the largest individual reduction. Fig. 2 was developed by implementing each strategy sequentially such that the CPU time reduction reported for each case represents the percentage of the original execution time achieved with

all the previous strategies also implemented (e.g., the time reduction reported for strategy 3 was obtained by simultaneous implementation of strategies 1–3). Each strategy and its impact on computation time are summarized below.

1) The largest reduction in computation time was achieved by utilizing finite elements of nonequal lengths, with each element continuing to have a single internal collocation point. Because the control horizon was much shorter than the prediction horizon, the length of the elements near the beginning of the prediction horizon remained at 2 min and the other element lengths were progressively increased to take advantage of the slowly changing dynamics near at the end of the prediction horizon. The total number of finite elements was reduced to 20, only one-sixth of the 120 elements used in the original NMPC controller. This strategy reduced the worst-case execution time by ~60% compared with the original controller.

2) The replacement of the full-order model with a compartmental model produced a significant reduction in the NMPC execution time, with a greater benefit achieved as the number of compartments was reduced. We believe that this trend was directly attributable to the conversion of differential equations to algebraic equations. Collocation was used to approximate the time derivatives in the ODEs as algebraic expressions involving the three collocation points (one internal point and one point on each finite element boundary) within the appropriate finite element. By contrast, collocation of an AE produced a discretized algebraic equation that depended only on the single collocation point at which the collocation was performed. As a result, AEs lead to more zero entries in the Jacobian matrix than the ODEs. By substantially increasing the number of algebraic equations while retaining the same total number of equations prior to collocation, model compartmentalization produced a sparser NMPC problem. Although the five-compartment model provided the greatest reduction in computation time, the resulting control performance was unacceptably poor for some production demand changes. Both the nine- and 15-compartment models produced good closed-loop performance which approached that obtained with the more computationally demanding full-order model. All the subsequent simulation results were generated with the nine-compartment model because it provided the best compromise between controller performance and computational effort. When combined with finite elements of nonequal length, the nine-compartment model produced a substantially smaller NLP problem (12 780 decision variables and 12 730 equality constraints) and reduced the worst-case execution time by ~75% compared with the original controller.

3) The NLP solver could be tuned for this specific application to further reduce the NMPC execution time. Despite being initialized with a nearly converged solution from the previous controller iteration, IPOPT generated iterative solutions that rapidly moved away from the initial guess before eventually returning to the converged solution after 15–20 unnecessary iterations. We solicited assistance from one of the IPOPT developers to adjust the solver options
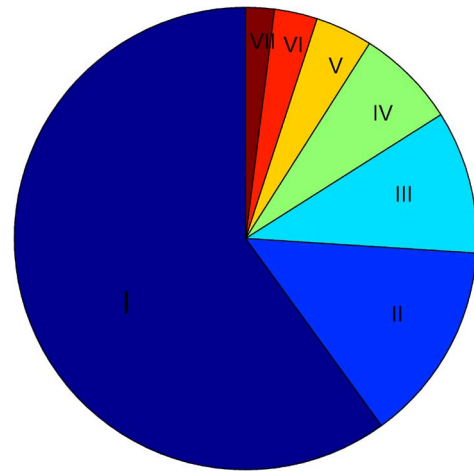

Fig. 2. Percentage reduction in the worst-case NMPC execution time achieved by sequential implementation of seven NMPC real-time implementation strategies following a change in the gaseous oxygen production rate demand. The strategies are numbered according to their relative impact on the execution time, where strategy 1 produced the largest individual reduction. The results were generated by implementing each strategy sequentially such that the CPU time reduction reported for each case represents the percentage of the original execution time achieved with all the previous strategies also implemented (e.g., the time reduction reported for strategy 3 was obtained by simultaneous implementation of strategies 1–3). The NMPC execution times for the original formulation without real-time implementation strategies and the final formulation with strategies I–VII were 40 and 2 min, respectively. Explanation of strategies: I—finite elements of nonequal lengths; II—nine-compartment model; III—IPOPT solver tuning; IV—analytical calculation of Jacobian and Hessian matrices; V—manual NMPC problem scaling; VI—NLP warm start; and VII—ramped setpoint changes.

for more rapid convergence than that obtained with the default solver options. Careful selection of the barrier parameter in the interior point algorithm proved to be particularly important for rapid convergence [30]. The combination of strategies 1–3 reduced the worst-case execution time by ~85% compared with the original controller.

4) The use of AMPL to analytically compute the Jacobian and Hessian matrices reduced numerical errors and improved convergence speed compared to numerical finite difference approximations. In addition to reducing the worst-case execution time by ~90% compared with the original controller, automatic calculation of derivative information does not require any additional effort by the user.

5) Although AMPL provides automated problem scaling to improve numerical stability and robustness, a small reduction in the worst-case execution time was achieved by manually scaling the NMPC variables and constraints prior to solution by AMPL.

6) A small reduction in worst-case CPU time was achieved by warm starting the NLP solver using the solution obtained at the previous time-step. This strategy only has a small impact immediately following a production demand change because the previous solution does not constitute a good initial guess of the current solution. By contrast, warm starting is essential for achieving rapid NMPC execution times during normal operation when the solution changes much more slowly at adjacent time-steps.

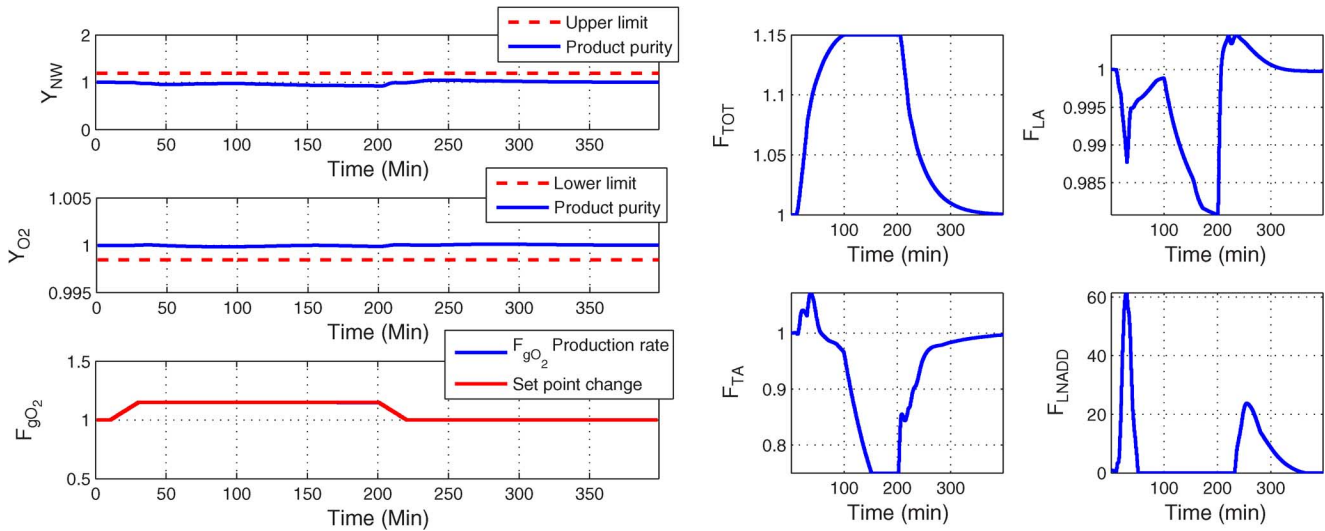7) In a final attempt to reduce the worst-case NMPC solution time, production rate changes were implemented as

Fig. 3. LMPC for $-/+15\%$ changes in the gaseous oxygen production rate demand. Input and output variables have been scaled such that their nominal values are unity.
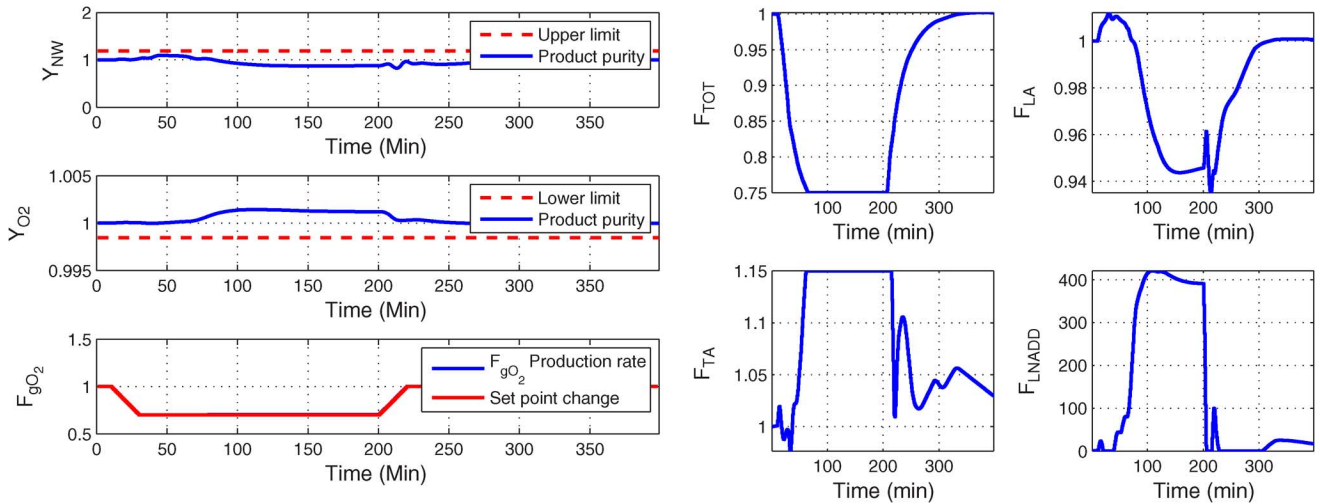

Fig. 4. LMPC for $-/+30\%$ changes in the gaseous oxygen production rate demand.

IV. CLOSED-LOOP SIMULATION RESULTS

To provide a reasonable basis for evaluating NMPC performance, linear model predictive control (LMPC) was used to design a linear constrained multivariable controller for the upper column. Using the manipulated inputs and controlled outputs listed in Table II and a sampling period of 1 min, a step response model was developed from simulation data generated by the full-order model through the application of standard system identification procedures used in the air separation industry. The effects of the total air flowrate were propagated to the upper column using the empirical linear models of the lower column described earlier. The LMPC objective function was chosen as in the nonlinear case (3) with the prediction and control horizons equal to 4 h $(P = 240)$ and 30 min $(M = 30)$, respectively. Explicit setpoints were used for the controlled outputs as in the NMPC controller. The step response model was posed as a set of linear equality constraints, and the objective function was minimized subject to the same inequality constraints used in the NMPC controller. A standard output disturbance model was used to eliminate steady-state offset. The resulting quadratic program (QP) was solved in Matlab using the solver `quadprog`.

The LMPC controller was evaluated for two series of ramped setpoint changes in the gaseous oxygen production rate demand (u_5^r) since the control objective is to satisfy the product composition specifications while changing the plant production rate. Setpoint changes in the product compositions are not meaningful as these specifications are not changed during normal plant operation. The first set of production rate demand changes
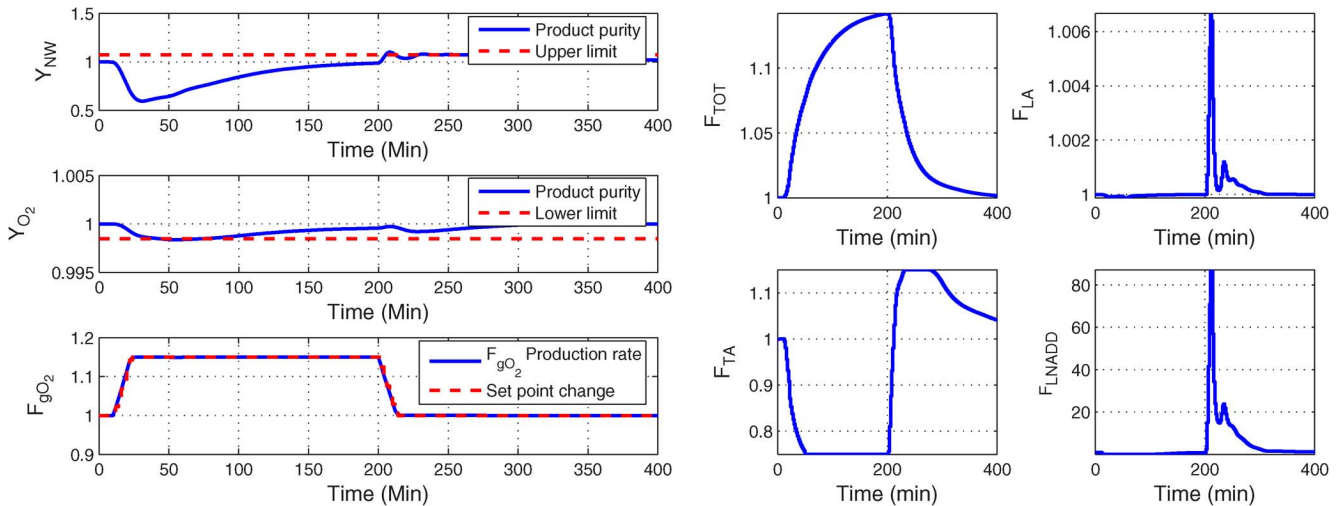
ramp inputs rather than step inputs. This strategy only had a small effect on the NMPC execution time and was not required for convergence of the NLP problem. The combination of strategies 1–7 reduced the worst-case execution time by $\sim95\%$ compared with the original formulation, yielding a NMPC controller that consistently converged within the 2-min controller sampling time.

Fig. 5.   NMPC for $+/-15\%$ changes in the gaseous oxygen production rate demand. Input and output variables have been scaled such that their nominal values are unity.

consisted of a setpoint increase of 15% followed by a setpoint decrease of 15% such that the demand was returned to its nominal value. The second set of demand changes consisted of a setpoint decrease of 30% followed by a setpoint increase of 30%. As with the NMPC controller, the LMPC objective function weights (q_j, r_j, s_j) were chosen by a trial-and-error tuning procedure to obtain satisfactory closed-loop performance. We experienced considerable difficulty obtaining feasible QP solutions and stable closed-loop performance due to large plant-model mismatch. Only a limited range of tuning parameters yielded acceptable performance, and this range was determined only after considerable effort. As compared to the NMPC tuning parameters, relatively large output weights on the two product purities and small input weights on the liquid air feed and the liquid nitrogen flowrates were required for acceptable performance. The resulting parameters are not reported here for the sake of brevity.

Fig. 3 shows the LMPC response for $\pm15\%$ changes in the gaseous oxygen production rate demand, with the input and output variables scaled such that their nominal steady-state values were unity to protect proprietary information. LMPC provided excellent setpoint tracking performance for these comparatively small changes. The use of relatively large output weights on the two product purities is clearly evident as the controller does not drive the column to the purity constraints, resulting in an unnecessarily high degree of separation. Fig. 4 shows the LMPC response for larger $\pm30\%$ changes in the production rate demand. Through painstaking controller tuning, we were able to obtain good setpoint tracking at the expense of large changes in the relatively expensive liquid air feed and the liquid nitrogen flowrates.

The NMPC controller was designed using the nine-compartment model as described in Section III-A and implemented using the real-time strategies discussed in Section III-B. NMPC was able to provide satisfactory tracking of small demand changes (Fig. 7). Despite transient prediction errors in the nine-compartment model used for controller design, NMPC was able to approximately satisfy the upper limit on the nitrogen waste purity and the lower limit on the oxygen product purity
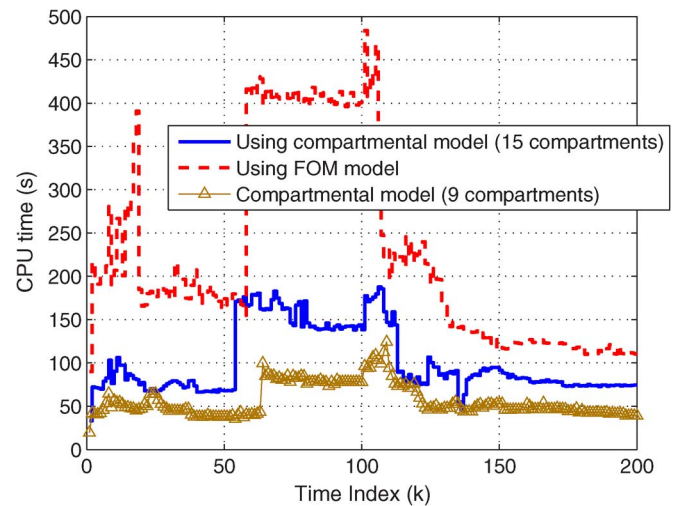

Fig. 6.   NMPC execution times at each sampling point for $+/-15\%$ changes in the gaseous oxygen production rate demand.

with only very small constraint violations. By contrast, LMPC was not able to drive the process to the purity constraints due to larger plant-model mismatch (Fig. 3). NMPC generated reasonable control actions and returned the relatively expensive liquid air feed and liquid nitrogen flowrates close to their nominal values following the second demand change. Even for these small demand changes, LMPC required larger moves in these expensive inputs to achieve acceptable performance (Fig. 3).

When the nine-compartment model was used for controller design, NMPC was able to consistently produce a converged control solution within the 2-min sampling interval (Fig. 8). The only exception was immediately following the second demand change, at which time the controller required approximately 125 s for convergence. More generally, relatively large execution times were obtained for several sampling intervals after a demand change because the warm start strategy was less effective under such highly transient conditions. As compared to NMPC controllers designed with the 15-compartment model
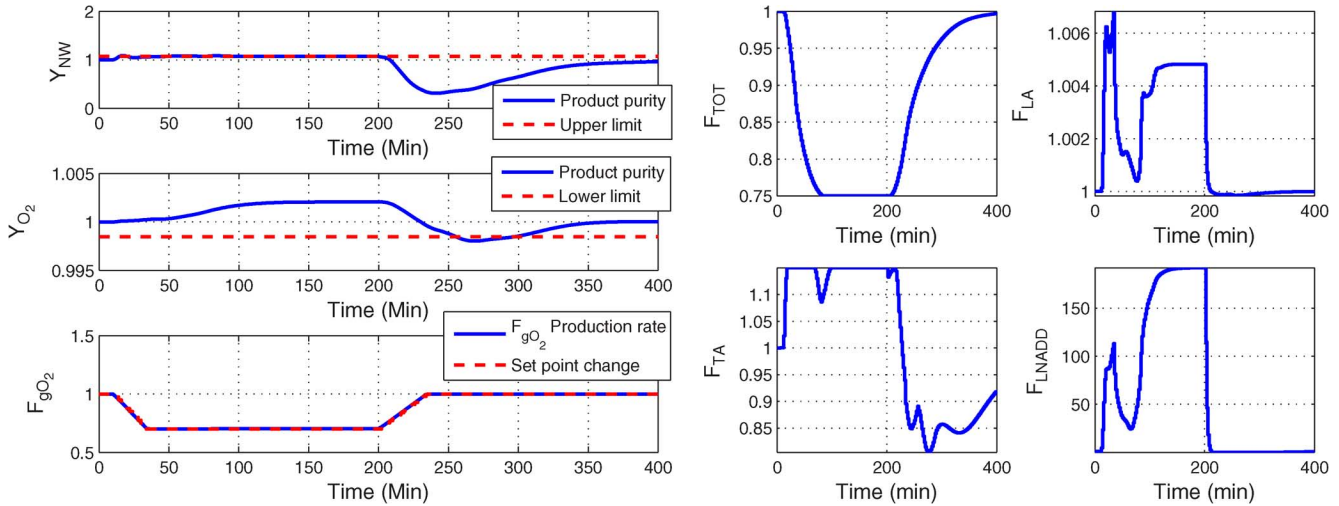
Fig. 7. NMPC for −/+30% changes in the gaseous oxygen production rate demand.

and the full-order model (FOM), the nine-compartment model provided significant reductions in NMPC execution times with little degradation in control performance (not shown).

The value of NMPC was more clearly evident for larger demand changes (Fig. 7). NMPC was able to effectively track the demand changes with reasonable control actions while driving the column to the purity constraints as necessary. While the purity constraints were only approximately satisfied due to plant-model mismatch, the only noticeable constraint violation occurring in the oxygen product purity following the second demand change. Although the control moves were less smooth than those generated for smaller demand changes (Fig. 5), controller behavior remained acceptable. The first demand change required the liquid air feed and liquid nitrogen flowrates to remain at elevated levels to satisfy the upper limit on the nitrogen waste purity. LMPC performance for the same demand changes (Fig. 3 was characterized by inability to drive the process to the purity constraints and much larger changes in the liquid air feed and liquid nitrogen flowrates, both of which translate to less effective column performance and higher operating costs.

For the larger demand changes, the nine-compartment model often produced similar NMPC execution times as the 15-compartment model. The primary advantage of the nine-compartment model was reduced execution times following the second demand change (Fig. 8), which allowed the NMPC controller to converge within the 2-min sampling interval. By contrast, the 15-compartment model required over 200 s immediately following this demand change. The full-order model (FOM) consistently required execution times exceeding the controller sampling interval, most notably over 400 s immediately following the second demand change. The reduced execution times obtained with the nine-compartment model were achieved with little degradation in control performance compared to the other two models (not shown). We found that NMPC simulations for +15% production rate increases consistently produced larger computation times than for −30% production rate decreases, regardless of the control model used. We hypothesize that the feasible region became smaller and the optimal solution moved closer to the boundary for the +15% production rate increase.
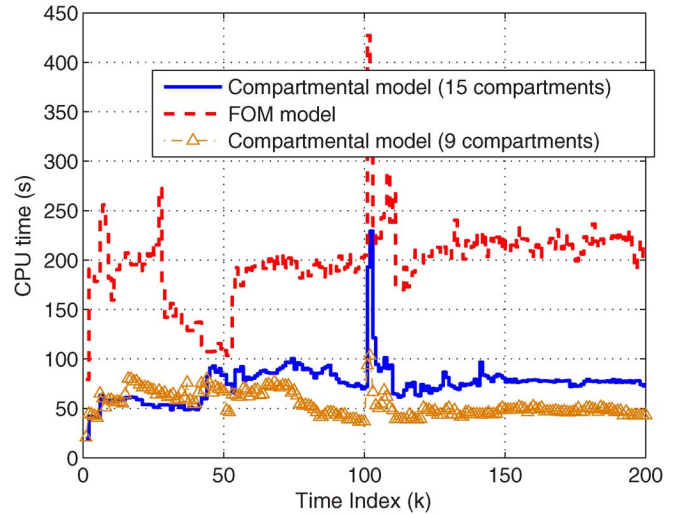

Fig. 8. NMPC execution times at each sampling point for −/+30% changes in the gaseous oxygen production rate demand.

This result is consistent with industrial experience that production rate changes approaching the maximum rate are more challenging than comparatively large production rate decreases.

V. SUMMARY AND CONCLUSION

A nonlinear model predictive control (NMPC) strategy has been developed for a prototypical distillation column in a cryogenic air separation plant to allow effective operation over a wide range of production rates. The controller design was based on a reduced-order nonlinear model derived from detailed mass and energy balances through compartmentalization and singular perturbation analysis. Temporal discretization of the compartmental model equations produced sparse Jacobian and Hessian matrices, which allowed more efficient solution of the NMPC optimization problem than was possible with the full-order balance model. To achieve consistent convergence of the NMPC problem within the 2-min controller sampling interval, several real-time implementation strategies including the use of nonequal finite elements over the prediction horizon

were required. Initializing the NLP solver with the converged solution at the previous time-step was found to significantly reduce NMPC execution times except immediately following a change in the production rate demand. The NMPC controller was shown to provide superior performance to a standard LMPC controller for large demand changes that exasperate column nonlinearities.

This study represents a first step towards the development of implementable NMPC technology for high purity distillation columns and other chemical process systems described by high-dimensional differential equation models. To assess the upper limits of achievable NMPC performance, the stage temperatures and compositions were assumed to be directly measurable. In practice, these state variables must be estimated from a sparse collection of noisy stage temperatures and product compositions. The present study focused on the upper column of a double column air separation plant. A more comprehensive approach will require integrated control of multiple columns and auxiliary processes including multistream heat exchangers and refrigeration equipment. We believe that the reduced-order modeling and real-time implementation strategies developed in this study should provide a valuable starting point for solving these considerably more challenging NMPC problems.

REFERENCES

[1] R. F. Barron, *Cryogenic Systems*.   New York: Oxford Press, 1985.
[2] W. H. Isalski, *Separation of Gases*.   New York: Oxford Press, 1989.
[3] A. Z. Meziou, "The application of multivariable constrained control to cryogenic air separation units," presented at the ISA Expo/2000, 2000.
[4] B. Roffel, B. H. L. Betlem, and J. A. F. de Ruijter, "First principles dynamic modeling and multivariable control of a cryogenic distillation process," *Comput. Chem. Eng.*, vol. 24, pp. 111–123, 2000.
[5] F. Allgower and A. Zheng, *Nonlinear Model Predictive Control*. Basel, Switzerland: Birkhauser, 2000.
[6] M. A. Henson, "Nonlinear model predictive control: Current status and future directions," *Comput. Chem. Eng.*, vol. 23, pp. 187–202, 1998.
[7] D. Q. Mayne and H. Michalska, "Receding horizon control of nonlinear systems," *IEEE Trans. Autom. Control*, vol. 35, no. 7, pp. 814–824, Jul. 1990.
[8] D. Q. Mayne, J. B. Rawlings, C. V. Rao, and P. O. M. Scokaert, "Constrained model predictive control: Stability and optimality," *Automatica*, vol. 36, pp. 789–814, 2000.
[9] L. T. Biegler, A. M. Cervantes, and A. Wachter, "Advances in simultaneous strategies for dynamic process optimization," *Chem. Eng. Sci.*, vol. 57, pp. 575–593, 2002.
[10] E. S. Meadows and J. B. Rawlings, "Model predictive control," in *Nonlinear Process Control*, M. A. Henson and D. E. Seborg, Eds.   Englewood Cliffs, NJ: Prentice-Hall, 1997, ch. 5, pp. 233–310.
[11] W. L. Luyben, *Process Modeling, Simulation and Control for Chemical Engineers*.   New York: McGraw-Hill, 1973.
[12] M. Diehl, H. G. Bock, J. P. Shloder, R. Findeisen, Z. Nagy, and F. Allgower, "Real-time optimization and nonlinear model predictive control of processes governed by differential-algebraic equations," *J. Process Control*, vol. 12, pp. 577–585, 2002.
[13] R. Huang, V. M. Zavala, and L. T. Biegler, "Traveling waves in chemical processes," *J. Process Control*, 2009, to be published.
[14] S. Bian and M. A. Henson, "Measurement selection for on-line estimation of nonlinear wave models for high purity distillation columns," *Chem. Eng. Sci.*, vol. 61, pp. 3210–3222, 2006.
[15] E. D. Gilles and B. Retzbach, "Reduced models and control of distillation columns with sharp temperature profiles," *IEEE Trans. Autom. Control*, vol. AC-28, no. 5, pp. 628–630, May 1983.
[16] W. Marquardt, "Traveling waves in chemical processes," *Int. Chem. Eng.*, vol. 30, p. 585, 1990.
[17] P. Seferlis and A. N. Hrymak, "Optimization of distillation units using collocation models," *AIChE J.*, vol. 40, pp. 813–825, 1994.
[18] C. L. E. Swartz and W. E. Stewart, "A collocation approach to distillation column design," *AIChE J.*, vol. 32, pp. 1832–1838, 1986.
[19] G.-Y. Zhu, M. A. Henson, and L. Megan, "Low-order dynamic modeling of cryogenic distillation columns based on nonlinear wave phenomenon," *Separation Purification Technol.*, vol. 24, pp. 467–487, 2001.
[20] S. Bian, S. Khowinij, M. A. Henson, P. Belanger, and L. Megan, "Compartmental modeling of high purity air separation columns," *Comput. Chem. Eng.*, vol. 25, pp. 2096–2109, 2005.
[21] J. Levine and P. Rouchon, "Quality control of binary distillation columns via nonlinear aggregated models," *Automatica*, vol. 27, pp. 463–480, 1991.
[22] S. Khowinij, M. A. Henson, P. Belanger, and L. Megan, "Dynamic compartmental modeling of nitrogen purification columns," *Separation Purification Technol.*, vol. 46, pp. 95–109, 2005.
[23] D. R. Yang and K. S. Lee, "Monitoring of a distillation column using modified extended Kalman filter and a reduced order model," *Comput. Chem. Eng.*, vol. 21, pp. S565–S570, 1997.
[24] A. Benallou, D. E. Seborg, and D. A. Mellichamp, "Dynamic compartmental models for separation processes," *AIChE J.*, vol. 32, pp. 1067–1078, 1986.
[25] P. V. Kokotovic, H. K. Khalil, and J. O'Reilly, *Singular Perturbation Methods in Control: Analysis and Design*.   Philadelphia, PA: SIAM, 1999.
[26] H. Michalska and D. Q. Mayne, "Moving horizon observers and observer-based control," *IEEE Trans. Autom. Control*, vol. 40, no. 6, pp. 995–1006, Jun. 1995.
[27] C. Rao, J. B. Rawlings, and D. Q. Mayne, "Constrained state estimation for nonlinear discrete-time systems: Stability and moving horizon approximations," *IEEE Trans. Autom. Control*, vol. 48, no. 2, pp. 246–258, Feb. 2003.
[28] S. Li and L. Petzold, "Software and algorithms for sensitivity analysis of large-scale differential algebraic systems," *J. Comput. Appl. Math.*, vol. 125, pp. 131–146, 2000.
[29] R. Fourer, D. M. Gay, and B. W. Kernighan, *AMPL: A Modeling Language for Mathematical Programming*.   Belmont, CA: Duxbury, 2002.
[30] A. Wachter and L. T. Biegler, "On the implementation of an interior-point filter line search algorithm for large-scale nonlinear programming," *Math. Prog.*, vol. 106, no. 1, pp. 25–57, May 2006.

Zhongzohu Chen received the B.S. and M.S. degrees in chemical engineering from Tianjin University, Tianjin, China, in 1993 and 1996, respectively, and the Ph.D. degree in chemical engineering from Cleveland State University, Cleveland, OH, in 2004.

He has held the position of Research Engineer at the Chemical Engineering Research Center, Tianjin University, from 1996 to 1999; Research Associate at the Center for Advanced Control Technologies and Industrial Technology Institute, Cleveland State University, from 2004 to 2005; Research Associate at the Center for Process Design and Control, University of Massachusetts, Amherst, from 2005 to 2006; and Polypropylene Process Engineer at Formosa Plastics, Point Comfort, TX, from 2006 to 2008. He currently is a Process Technology Engineer with Bayer Technology Services Americas, Baytown, TX. His work is focused on advanced process control, dynamic simulation, and process optimization.

Michael A. Henson (SM'04) received the B.S. degree in chemical engineering from the University of Colorado, Boulder, in 1985; the M.S. degree in chemical engineering from the University of Texas, Austin, in 1988; and the Ph.D. degree in chemical engineering from the University of California, Santa Barbara, in 1992.

He has held the position of Visiting Research Scientist with the DuPont Company from 1992 to 1993; Assistant Professor and Associate Professor of chemical engineering at Louisiana State University, Baton Rouge, from 1994 to 2002; Alexander von Humboldt Research Fellow with the University of Stuttgart, Stuttgart, Germany, from 2001 to 2002; and Visiting Professor with the Harvard Department of Systems Biology in 2009. He currently is a Professor of chemical engineering, Director of the Center for Process Design and Control, and Co-Director of the Institute for Massachusetts Biofuels Research at the University of Massachusetts, Amherst. His research is focused on nonlinear modeling and control of chemical and biotechnological processes.

Paul W. Belanger received the B.S. degree in chemical engineering from Villanova University, Villanova, PA, in 1993, and a Ph.D. degree in chemical engineering from Lehigh University, Bethlehem, PA, in 1997.

He has held the positions of Senior Engineer with The BOC Group from 1997 to 1998 and Lead Engineer with Kesler Engineering from 1998 to 2000. From 2000 through 2009, he has been employed by Praxair, Inc., Tonawanda, NY, where he has held the positions of Development Associate, Program Development Manager, and is currently the Senior R&D Manager of the Adsorption Process and Systems Group.

Larry Megan received the B.S. degree in chemical engineering from Worcester Polytechnic Institute, Worcester, MA, in 1988, and the Ph.D. degree in chemical engineering from the University of Connecticut, Storrs, in 1993.

He has worked with Praxair Research and Development, Tonawanda, NY, since 1993. He is currently a Corporate Fellow and manages Praxair's Advanced Control and Operations Research R&D Group. The group specializes in using advanced computational methods to maximize the effectiveness of its chemical and manufacturing operations.